International Journal on Recent and Innovation Trends in Computing and Communication
ISSN: 2321-8169 Volume: 11 Issue: 9
Article Received: *25 July 2023* ***Revised:*** *12 September 2023* ***Accepted:*** *30 September 2023*

Investigation of Enhanced Performance in Flexible Solar Cells Using Passive Cooling Technique

Lalit Jyani[1*], Sunil Kumar Sankhala[2], Kailash Chaudhary[1] and Kamlesh Purohit[1]

[1]Department of Mechanical Engineering,
MBM University.
Jodhpur, India 342001
Corresponding Author - jyani.lalit809@gmail.com
[2]Defence Laboratory,
DRDO Jodhpur, India 342001
ssunil.dl@gov.in
[1]Department of Mechanical Engineering,
MBM University.
Jodhpur, India 342001
k.chaudhary.mech@gmail.com
[1]Department of Mechanical Engineering,
MBM University.
Jodhpur, India 342001
Kpurhohit.mech@jnvu.edu.in

Abstract: The lack of flexibility and enormous weight in conventional photovoltaic (PV) modules limits their applications. The advantages of flexibility and lightweight have made flexible solar cells popular in various applications. However, flexible PVs have an efficiency degradation due to an increase in module temperature through incoming solar infrared radiation. Both the power output and the electrical efficiency of the PV module depend linearly on the operating temperature. For every degree increase in the PV temperature, the efficiency decreases by 0.45-0.65%. Here, the novel concept of applying a nanomaterial-based heat-resistant coating for the passive cooling of flexible solar cells was experimentally investigated. A heat-resistant coating generally keeps buildings cooled by filtering UV and infrared rays and transmitting visible rays. This approach works by controlling the incoming solar radiation, thereby decreasing the overall temperature of flexible solar cells passively without adding much weight. Here, a transparent flexible polyacrylic sheet 0.25 mm in thickness was used, and two coats of silver nanomaterial-based coating were applied. The sheet was placed over a flexible solar photovoltaic module with a power rating of 6 watts. The temperature of the flexible solar photovoltaic module was recorded at different time intervals for August, September, and October using temperature sensors, taking note of factors such as wind speed and solar irradiation. These readings were compared with those taken from the solar panel without any coating. A temperature reduction of 6-7°C and an improved solar power efficiency of 2.5-4 % were observed for cooled flexible solar panels.

Keywords- Photovoltaic flexible module, nanomaterial coating, polyethylene transparent acrylic sheet, Passive cooling.

1. Introduction

1.1 Effect of temperature on PV solar cells

The operating temperature is an important factor that affects the efficiency of photovoltaic solar cells. The increased temperature of the solar cell influences the current and voltage. The I-V curve of photovoltaic panels shows that the current and voltage linearly depends upon the temperature [1]. For every degree of increase in the solar cell temperature, crystalline solar cells decrease the efficiency by 0.45-0.65% [2]. There is a similar effect in flexible solar cells, which are highly sensitive to an increase in temperature. Therefore, reducing the solar cell temperature can directly enhance its efficiency and improve its overall life.
Many researchers have worked on the cooling of solar cells, in

International Journal on Recent and Innovation Trends in Computing and Communication
ISSN: 2321-8169 Volume: 11 Issue: 9
***Article Received:** 25 July 2023 **Revised:** 12 September 2023 **Accepted:** 30 September 2023*

which the cooling of flexible and rigid solar cells by the active cooling [3] method was widely studied. However, active cooling is not a recommended method because it increases the overall bulkiness of panels and contains moving parts; therefore, active cooling is not a feasible method for reducing solar cell temperature. To overcome this problem, many researchers have studied passive cooling techniques to reduce the working temperature of solar cells without adding much weight [3].

1.2 Literature Survey

Several researchers have worked on cooling PV panels via different approaches, including both active and passive cooling techniques. Air circulation is one of the simplest and most natural methods for cooling solar cells, and to enhance convective heat transfer, fins are used to enhance the heat transfer area. Edenburn [4] developed a device made up of linear fins fitted on all available heat sink surfaces that are used for passively cooling single cells. Araki [5] worked on passive cooling technologies for solar cells and reported that good thermal conduction between cells and heat-spreading plates was important.

Tonui [6] and Kalogirou [7] reported their experiments on modified PV/T collectors, and the results showed that maximum temperature reduction can be achieved by natural ventilation and forced ventilation. As a cooling media, water in different forms has been widely used for PV cooling and is suitable for PV/T systems.

Tripanagnostopoulos [8] compared the electrical efficiency of PV/water, PV/air, and PV/free systems and of PV/insulation under an ambient air temperature of 29°C. It was concluded that a maximum efficiency increase of 3.2% was achieved with PV/water.

Krauter [9] investigated the method of cooling PV modules with a water film flowing on the top surface. With the additional evaporative heat transfer, it was claimed that they could decrease the cell temperature up to 22°C and obtain a net increase in electrical efficiency from 8 to 9%.
Hadipour [10] and Kordzadeh [11] studied the use of water spray to cool PV panels and achieved an increase in the efficiency of solar cells [11].

Cuse [12] experimentally studied polycrystalline PV cells under controlled conditions in which the illumination was varied from 200 to 800 W/m^2. He used two PV cells: one with aluminum fins as a heat sink, one with thermal grease applied, and the other without a heat sink. A relative increase in electric efficiency of 9% was observed via the use of passive cooling with a heat sink.

R. M. Hernandez [13] showed that the depth of the air channel between PV cells and roofs has a significant influence on cooling, and the PV module temperature difference is 5-6°C when compared with that of a PV module on a regular mount. [14-18] showed that with the right type of PCM material, a decrease in the temperature relative to the reference PV cell can be achieved. The power gain was greater than that of the reference PV module. Several studies have been performed on front and back cooling[3].

Rosa-Clot [17] used a submerged technique to cool down a monocrystalline PV module with water.

El-Seesy [18] attempted to cool PV cells via the thermosyphon effect. The increase in relative efficiency gained was 19%.

Chandrasekar [19] and Alami [20] used the capillary effect to cool down the back of a monocrystalline PV module with a 0.36 m2 surface area. The capillary effect was produced via cotton wick structures wrapped spirally at the back of the module and immersed in the fluid. The maximum increase in efficiency reaches 10.4% when compared to that of a noncooled module. [20]
Han [21]compared the cooling of CPV solar cells operated in deionized (DI) water, isopropyl alcohol (IPA), dimethyl silicon oil, and ethyl acetate. In the experiment, an increase in efficiency of 8.5–15.2% was achieved.

Abdulgafar [22] studied the efficiencies of 0.12 W and 15 cm^2 polycrystalline PV cells immersed in deionized water at different depths. An increase in efficiency was observed with increasing water depth, with a maximum value for an efficiency of approximately 22% occurring at a depth of 6 cm.

Lu [23] designed and fabricated ultrabroadband texture imprinted glass-to-silicon PV modules. Optical tests demonstrated that the silica texture exhibited a higher transmittance within the visible-near infrared wavelength band than did commonly used glass, which improved the effective optical efficiency of solar cells and correspondingly improved the electrical efficiency.

Zhou [24] demonstrated enhanced radiative cooling for low-bandgap PV cells under showed that the operating temperature of solar cells was passively reduced by 10°C, corresponding to a relative open-circuit voltage improvement of 5.7%.

International Journal on Recent and Innovation Trends in Computing and Communication
ISSN: 2321-8169 Volume: 11 Issue: 9
Article Received: *25 July 2023* ***Revised:*** *12 September 2023* ***Accepted:*** *30 September 2023*

2. Description of the experimental setup

Here, the experimental setup consists of a 4-cell flexible solar panel with a wattage of 6W, and the cells are connected in series as shown in Fig 1. The solar panel is kept at a 31° tilt angle [25] to obtain the maximum radiation at 26.2697°N and 73.0352°E. Two coats of silver nanomaterial coating with a thickness of 1.5 mils (38 microns Approx.) each were applied on the acrylic sheet by a roller. A Positest DFT dry film thickness gauge measured the thickness of each coating. The size of both solar panels is 52.5 cm × 13.5 cm, as shown in Fig. 2.

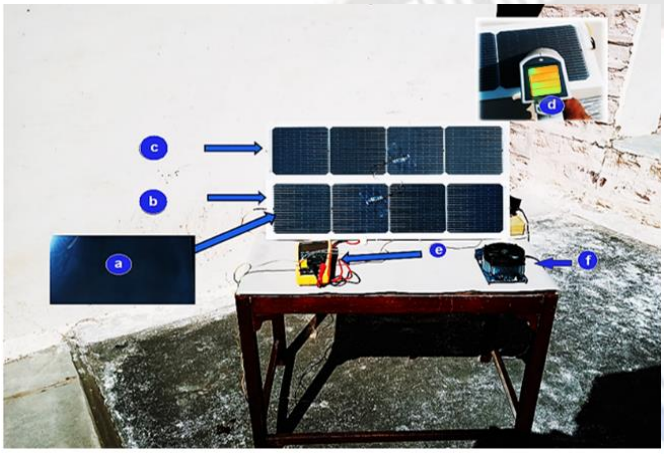

Figure 1. Actual Flexible PV Setup **(a)** Transparent thin film, **(b)** flexible solar panel (with coated transparent thin film), **(c)** flexible solar panel (without coated transparent thin film), and **(d)** Thermal camera (fluke)) **(e).** Multimeter (DM 97) **(f)** Load Circuit

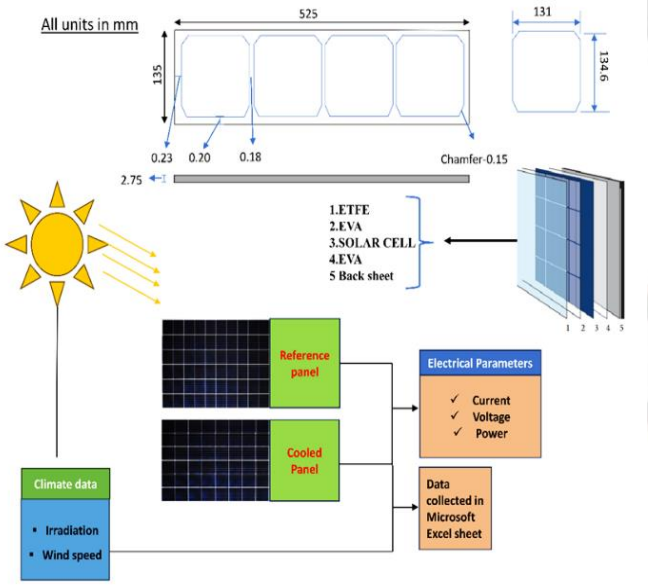

Figure 2. The systematic layout of the experimental setup

2.1 Specification of Data Collection Instruments

The main features of the instruments used in the installation are shown in Table 1. The PV panel temperatures are measured with an IR temperature thermometer and flexible resistance temperature detectors (RTD), which are attached to the front of the panel (panel 1 i.e. Reference panel, panel 2 i.e. cooled panel). Also, load circuit, multimeter, pyranometer, and other instruments were used for data collection with minimal error.

2.2 Preparation of the coating

Silver-based heat-resistant coatings were directly applied to acrylic sheets with 82% transparency [26] and 0.25 mm thickness with the help of a 7-inch bubble pattern sponge roller. The second coat was applied after the first coat, after a duration gap of 6 hours. After drying the second coating, a thickness meter was used to measure the thickness of the final coating. The acrylic sheets before and after coating are shown in Fig. 3a and Fig. 3b, respectively.

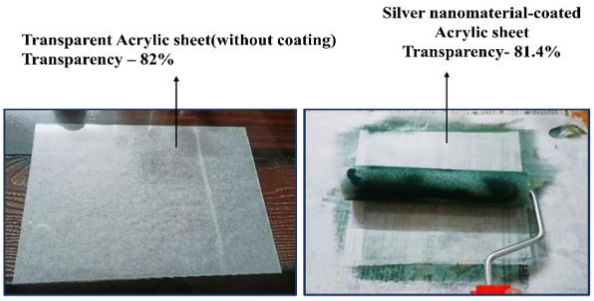

Figure 3. (a) Transparent acrylic sheet with a thickness of 0.25 mm. **(b)** Silver-based heat-resistant coating performed by a sponge bubble patterned roller (placed over biodegradable paper).

2.3 Characteristics of the nanocoating and instruments used in the experiment

2.3.1 Low-emissivity nanocoating

The emissivity is the ratio of heat emitted from a given material to that emitted from a blackbody and ranges from zero to one [27]. A blackbody would have an emissivity of 100%, and a perfect reflector would have a zero value. The emissivity of the surface of a material is its effectiveness in emitting energy as thermal radiation. The typical emissivity of common materials is listed below in Table 2.

Table 1. Description and specification of instruments used in Experimentation

Parameters	Values
Thermal camera (fluke VT-08)	
Temperature range	–20°C to +120°C
Resolution	320 X 340 pixels
Thermal sensitivity	< 0.05°C @ +30°C/50 mK
Measuring accuracy	±2°C or ±2% of reading
Electronic Load(cool master 150)	
Range	0–100 V /0–10 A
Accuracy	±5 mV ±5.4 mA
Multimeter-HTC (with temperature sensor)	
Accuracy	(23±5)^{o}C
Ac Current	± (1.5%10)
AC voltage (true RMS)	± (1.0%+5) for 400mV
	±(0.8%=10d) for 4V,40V,400V
Frequency	± (0.4%+4)
Temperature range	+40^{o}C~1000^{o}C
Temperature accuracy	< 400^{o}C ± (0.8%+4)
	>400^{o}C± (1.5%+15)
Pyranometer	
Make	EKO MV-01
Power consumption	9W
Operating temperature range	-30 - 60^{o}C
Induced Zero offsets	< W/m^2
Maximum operational irradiance	4000 W/m^2
Response time (95%)	< 0.5s

International Journal on Recent and Innovation Trends in Computing and Communication
ISSN: 2321-8169 Volume: 11 Issue: 9
***Article Received:** 25 July 2023 **Revised:** 12 September 2023 **Accepted:** 30 September 2023*

Table 2. The emissivity of common materials [26]

S.No	Materials surface	Thermal emissivity
1	Aluminium foil	0.03
2	Asphalt	0.88
3	Brick	0.90
4	Concrete, rough	0.91
5	Glass, smooth (uncoated)	0.91
6	Limestone	0.92
7	Marble, Polished, or white	0.89–0.92
8	Marble, Smooth	0.56
9	Paper, roofing, or white	0.88–0.86
10	Plaster, rough	0.89
11	Silver, polished	0.02
12	Silver Nanomaterial Coating	0.0035

Heat Resistant coating as shown in Fig. 4 is an advanced nanotechnology-based transparent liquid glass coating that insulates the glass, by effectively filtering up to 99.9% UV & 80- 90% of IR rays emitted by the sun while still allowing up to 80% of the visible light to penetrate through the glass. The nanocoating is a low emissivity coating [27] technology and a cost-effective solution for energy saving used for coating windows of buildings. The applied low-E coating is a silver-based coating that filters UV and IR radiation as these radiations act in heating the solar panel, leading to a decrease in the power conversion efficiency.

Figure 4. Silver-based nano-coating [26]

2.4 Instruments

2.4.1. Thermal Camera

A noncontact fluke VT-08 thermal camera shown in Figure 5a. was used to capture the temperature profile of the solar panel. Its features include an optically matched coaxial laser sight system designed to precisely and accurately outline the target measurement area.

Figure 5. (a) Fluke thermal camera **(b)** Electronic load circuit **(c)** Pyranometer

2.4.2. Digital Multimeter, Pyranometer and Load Circuit

A digital multimeter HTC DM-97 was used to measure the current-voltage characteristics. The accuracy and temperature range of the multimeter were (23±5)ºC and +40ºC~ 1000ºC, respectively. A 150 W-20A electronic load circuit shown in Fig. 5b. was used to apply different loads to plot the current-voltage characteristic curves for the coated and uncoated panels. The radiation data was collected using an EKO MV-01 pyranometer as shown in Fig. 5c.

3. Experimental procedure

A silver-based coating was used for coating acrylic sheets of 0.25 mm thickness. The dimensions of the sheets were equal to the thickness of the flexible solar module. The coating was performed with the help of a sponge roller over the film, and two coats were applied with a time interval of 6 hours between the coats. The coated acrylic sheet was placed over the flexible solar module with an optimum tilt angle of 31°, and the experiment was conducted at a location with 26.2697° N latitude and 73.0352° E longitude [25]. The readings were taken using ASTM standards [28] from 10:30 am to 4:30 pm daily on the 15th day for three months, i.e., August, September, and October. The instrumental error was considered negligible. A multimeter HTC DM-97 was used to measure the current and voltage of the panel at different time intervals. A Raytek Raynger MX2 infrared thermometer was used to measure the surface temperature with and without coating for different time intervals during the day and for the months from August to October. The specification of flexible PV panels is shown in Table 3.

Table 3. Flexible PV panel specification.

Parameters	Values	Parameters	Values
Pmax	6 W	Short-circuit current I_{SC}	0.91 A
Voltage at Pmax (V_{MP})	6.8 V	Voltage temperature coefficient (V_M)	-0.3%/ºC
Current at Pmax (I_{MP})	0.88 A	Current temperature coefficient (I_M)	+0.1/ °C
Open-circuit voltage (V_{OC})	7.2 V	Power temperature coefficient (P_M)	-(0.5±0.05)/ºC

3.1 Experimental environment

The experiment was conducted during August, September, and October on the 15th day of these months. Figure 6. shows the horizontal global radiation on the 15th day of August,

International Journal on Recent and Innovation Trends in Computing and Communication
ISSN: 2321-8169 Volume: 11 Issue: 9
Article Received: *25 July 2023* ***Revised:*** *12 September 2023* ***Accepted:*** *30 September 2023*

September and October for the time interval between 10:30 am and 4:30 pm. The curve depicts approximately the same behaviour except for some distortions in August and September due to cloudiness. The solar radiation during August was slightly lower compared to September due to cloudiness and other atmospheric conditions. The radiation intensity during noontime was as high as 700 W/m2. Temporal variations were also observed due to changes in the wind speed ranging from 7 to 10 km/hr. The standard testing condition (STC)[29] of the solar panel is performed at a temperature of 25°C, irradiation of 1000 watt m^{-2}, and an air mass index (AM) of 1.5.

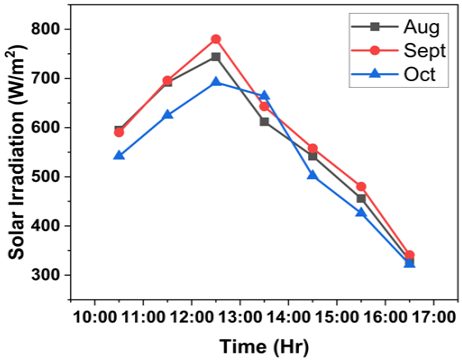

Figure. 6. Irradiation in August, September, and October

3.2 Effect of cool coatings on the temperature of flexible solar cells

Silver-based cool coatings [30] generally keep buildings cool by filtering out UV and infrared rays and transmitting visible rays. Here, the same effect was also shown for flexible solar panels, where a thin transparent film of silver-based coating was placed over flexible solar panels. The coating acts as an optical filter, transmits visible light and reflects infrared and ultraviolet radiation, which passively cools the solar panel. The cool coating reduces the temperature of flexible solar cells by controlling the incoming solar radiation, thereby enhancing the overall performance of solar panel.

3.3 Electrical Performance

The electrical improvement of the panel due to the reduction in the temperature can be evaluated by the temperature coefficient of voltage, as shown in Table 3., which is 0.3%/°C [31]. When the temperature of the flexible PV panel decreases, the open-circuit voltage also increases, and vice versa. Figure 10 shows the comparison between cooled panels using a coated thin film and noncooled panels without a coated film. It clearly shows that for the cooled panel, the open-circuit voltage is higher than that for the noncooled panel. The variation in open-circuit voltage is due to variations in atmospheric conditions, i.e., winds and clouds.

The efficiency of solar panels can be calculated by the Evans–Florschuetz PV efficiency correlation.

$$\eta_{ref(PV)}[1-\beta_{ref}(T_{pv}-T_{ref})] \quad (1)$$

where η_{ref} is the reference efficiency, T_{ref} is the reference temperature of the PV cells, T_{pv} is the temperature of the PV cells, and β is the temperature coefficient of efficiency of the PV cells Based on the data listed in the Evans–Florschuetz thermal model [1], T_{ref} = 25°C, average $\eta_{ref(PV)}$ = 0.15 and average β_{ref}=(0.0041)° C^{-1} for a-si were used.

$$\text{Improvement}\,\% = 100 * \frac{\eta_{\text{Cooled PV}} - \eta_{\text{reference PV}}}{\eta_{\text{reference PV}}} \quad (2)$$

Here, η_{ref} and β_{ref} are given by the PV manufacturer. The percentage improvement in electrical efficiency is due to passive cooling. The expression for efficiency improvement can be written as [32].

Fig. 7. shows the ambient air temperature on the same day for August, September, and October. The ambient temperature in September was the highest, exceeding 38°C, while for August and October, it was approximately 37°C at midday. Due to the rainy season in August, where maximum rainfall is recorded, the temperature does not increase as clouds remain for maximum hours.

3.4 Experimental Uncertainty Assessment

In any experimental work, there is the potential to encounter some level of errors that may arise from the measurand or the measurements [33]. In mathematics if there are N number of observations and x_i denotes any of the observations (where i can have any integer value beginning from 1 to N), the mean which in this case is denoted by x can be calculated using Eq. (3).

$$\bar{x} = \frac{x_1+x_2+\cdots+x_N}{N} = \frac{1}{N}\sum_{i=1}^{N} x_i \quad (3)$$

In experimental works, it is important to quantitatively assess how much each measurement scatter about the mean. The level of scatter about the mean value helps in identifying the level of

International Journal on Recent and Innovation Trends in Computing and Communication
ISSN: 2321-8169 Volume: 11 Issue: 9
Article Received: *25 July 2023* ***Revised:*** *12 September 2023* ***Accepted:*** *30 September 2023*

precision of the experimental results, and as a result assist in the quantification of the random uncertainty. The standard deviation (SD) is the most accepted quantitative measure of scatter. The SD can be calculated using Eq. (4) for cases that have data points with equal weight [34].

$$SD = \sqrt{\frac{\sum_{i=1}^{N}(x_i - \bar{x})^2}{N-1}} \qquad (4)$$

the experiment was conducted is as shown in Figure 1. It can be observed from the figure that the temperature of the uncooled panel reached its peak between 12:00 pm and 1:00 pm. This can be attributed to the high ambient temperature recorded during that period of the experiment as indicated in Figure 7. The cooled panel was however able to maintain some level of stability relative to its temperature due to the effectiveness of the cooling mechanism. The temperatures of both panels however started reducing after 1:30 pm due to a sharp drop in the ambient temperature occasioned by cloud formation which also affected the intensity of the solar radiation. According to the results, the cooled system recorded an average temperature of 35.72 ◦C while the uncooled system recorded an average temperature of 59.27 ◦C. The difference in temperature between the two panels averagely is 23.55 ◦C. It can be observed from the figure that, the temperature of the cooled panel was slightly higher than the uncooled panel at the beginning of the experiment, obviously due to the fact that, the cooled panel was deficient of natural air at the rear side of the panel, because of both the cotton wick mesh and the aluminum sheet at its back. As a result, the uncooled panel was being cooled by the ambient air which at the start of the experiment was relatively colder. The SD for the uncooled panel was relatively high compared to the cooled system, the uncooled panel recorded 11.57 against 2.47 for the cooled system. Similarly, the uncertainty for the uncooled system was 3.21 against 0.69 for the cooled system. These large uncertainties can be associated with the sharp rise in the ambient

The SD provides the estimate for the random uncertainty for any one of the values used in calculating the SD. The SD of the mean value for a number of measurements σ_m with equal statistical weights can be calculated using Eq. (5), the σ_m is the uncertainty [34].

$$\sigma_m = \sqrt{\frac{\sum_{i=1}^{N}(x_i - \bar{x})^2}{N(N-1)}} = \frac{SD}{\sqrt{N}} \qquad (5)$$

4. Results and discussion

4.1 Temperature of the flexible PV panel

Outdoor experiments on flexible solar panels were conducted on the 15th day of every month for three months, and the results from the panels with coating and

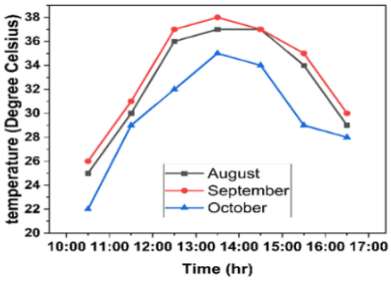

Figure 7. Ambient temperature in August, September, and October

without coating were obtained, and the temperature of the panels was recorded. Fig. 8 shows the temperature of flexible solar panels with and without coated acrylic sheets between 10:30 am and 04:30 pm on the 15th of August, September, and October months. The red curve represents the temperature variation for the cooled panel with coated acrylic sheets, and the blue curve represents the temperature variation for the panel without coating. At the start of the experiment, the temperature of both panels increased to a maximum and then started to decrease as the sun's position changed during the day. The minimum temperature is recorded for both panels initially and then starts increasing as the sun moves toward the east to west. The temperature of the cooled panel, i.e., the panel with a coated transparent film, is lower than that of the panel without a coated film. The average difference between the two panels is 4°C, and it reaches 6-7°C for some instances.

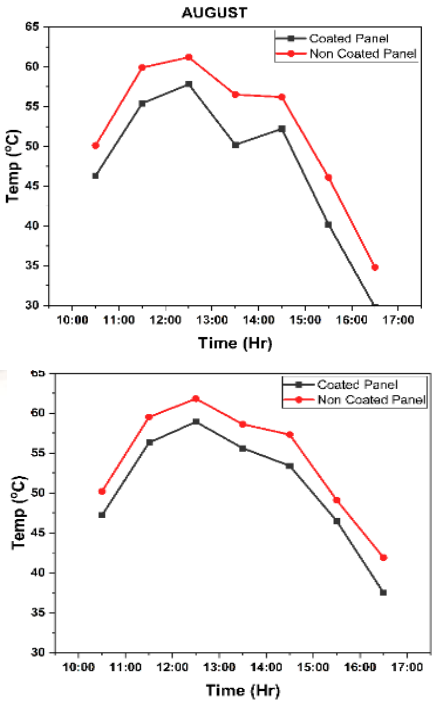

International Journal on Recent and Innovation Trends in Computing and Communication
ISSN: 2321-8169 Volume: 11 Issue: 9
Article Received: *25 July 2023* ***Revised:*** *12 September 2023* ***Accepted:*** *30 September 2023*

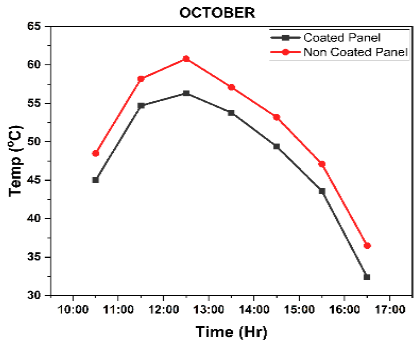

Figure 8. Temperature comparison of two panels in the months of (a) August (b) September (c) October

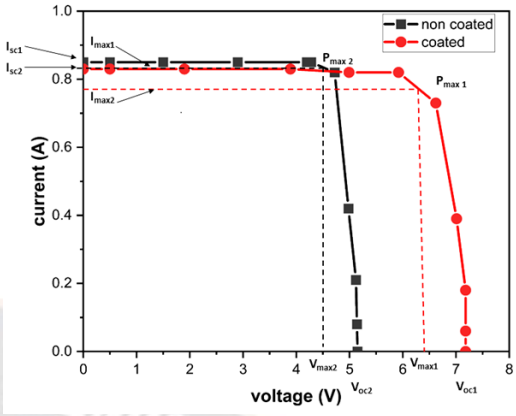

Figure 9. I-V Curve Characteristics for Two Panels for month of August

4.2 I-V Characteristics of the PV Panel

The short-circuit current and open-circuit voltage of flexible solar panels with and without coating are shown in Fig. 9. Initially, the short-circuit current remains nearly constant for both the cooled and noncooled panels. With the increasing load in the form of resistance and after the maximum peak point, the load starts to fall where the voltage is at its maximum and the current is zero. Table 4. shows the maximum current value, i.e., Imax, is 0.78 A and 0.82 A for the coated and noncoated panels, and the corresponding values for Pmax are 5.05 and 3.69, respectively. The maximum voltage is 6.48 V for the coated panels and 4.50 V for the noncoated panels. The above curve is plotted at an irradiation of 744 W/m^2 for the 15th day of August. Similar characteristics can be found for different sun intensities for different months. There was an improvement in the efficiency of approximately 2 % for the cooled panel due to an increase in voltage by unit value.

As temperature increases, the current produced by a solar panel can also increase slightly. This is due to the increased mobility of charge carriers i.e electrons within the solar cells, resulting in a higher current output. Similarly, an increase in temperature typically reduces the open-circuit voltage of a solar cell. This decrease is because as the temperature rises, more electron-hole pairs are generated, which increases the leakage current. This increased leakage current results in a lower voltage across the solar cell terminals. Consequently, the net result of these changes is often a reduction in the overall power output of the solar panel. This is because the decrease in voltage typically has a larger impact on power output compared to the slight increase in current. Therefore, the cooled panel has better electrical efficiency compared to the noncooled panel. The efficiency of the photovoltaic panel can also be calculated using the following formula:

$$\% \text{ Efficiency} = \left(\frac{\text{Power output of PV cell}}{\text{Power input from the sun}}\right) \times 100 \qquad (6)$$

$$\% \text{ Efficiency} = \left(\frac{\text{Voc} \times \text{Isc} \times \text{fill factor}}{\text{Cell area} \times 1000}\right) \times 100 \qquad (7)$$

Table 4. Experimentally calculated values for P_{max}, $I_{max,}$ and V_{max}

Parameters	Modules		Results
	Coated	Non coated	
Pmax	5.05	3.69	% increase in P_{max} = 36.85
Imax	0.78	0.82	% decrease in I_{max} = 4.8
Vmax	6.48	4.50	% increase in V_{max} = 44

4.3. Thermal characteristics of the panel and weather conditions

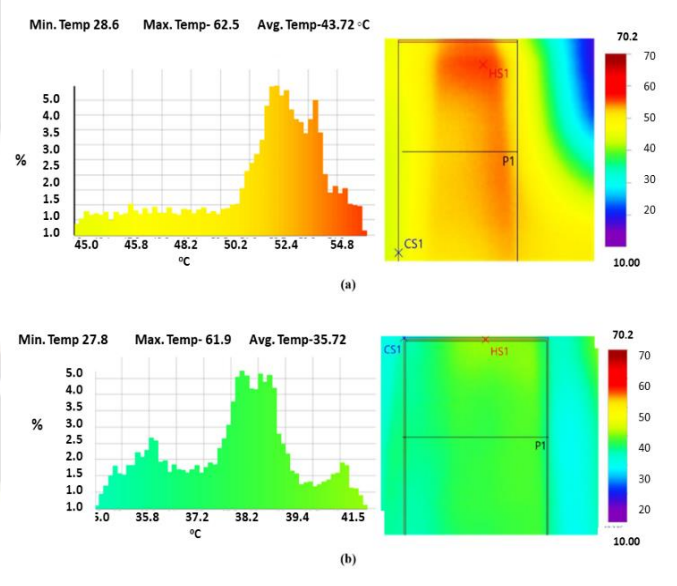

Figure 10. Temperature distribution histogram and thermal images for the (a) uncooled panel (b) cooled panel.

The solar radiation and the ambient temperature were recorded from 10:30 am to 4:30 pm within a 60-minute interval and the results are presented in Figure 6 and Figure 7. As can be seen from the figure, the solar radiation for the day was at its peak around 12:30 pm pm, mostly this should have been around 12

International Journal on Recent and Innovation Trends in Computing and Communication
ISSN: 2321-8169 Volume: 11 Issue: 9
***Article Received:** 25 July 2023 **Revised:** 12 September 2023 **Accepted:** 30 September 2023*

pm but around that time, there was some little cloud formation which may have affected the solar irradiation around mid-day. The day recorded an average solar irradiation of 582 W/m^2. The average ambient temperature for the day is also around 28.28 ^{o}C with the highest temperature of about 37.8^{o}C occurring at about 1:30 pm.

The temperature for the two panels was obtained by finding the average of the temperatures recorded by each thermocouple installed at the front side of the two panels for each 60-minute interval. The results for the temperature distribution for the period within which the experiment was conducted are shown in Figure 8. It can be observed from the figure that the temperature of the uncooled panel reached its peak between 12:00 pm and 1:00 pm in August, September, and October respectively. This can be attributed to the high ambient temperature recorded during that period of the experiment as indicated in Fig. 7. The cooled panel was however able to maintain some level of stability relative to its temperature due to the effectiveness of the cooling mechanism. The temperatures of both panels however started reducing after 1:30 pm due to a sharp drop in the ambient temperature occasioned by cloud formation which also affected the intensity of the solar radiation. According to the results, the cooled system recorded an average temperature of 35.72 ◦C while the uncooled system recorded an average temperature of 43.27 ◦C. The difference in temperature between the two panels averagely is 6-7 ◦C. It can be observed from the figure that, the temperature of the cooled panel was slightly higher than the uncooled panel at the beginning of the experiment, obviously due to the fact that, the cooled panel was deficient of natural air at the rear side of the panel. As a result, the uncooled panel was being cooled by the ambient air which at the start of the experiment was relatively colder. The SD for the uncooled panel was relatively high compared to the cooled system, the uncooled panel recorded 6.57 against 1.38 for the cooled system. Similarly, the uncertainty for the uncooled system was 1.21 against 0.28 for the cooled system. These large uncertainties can be associated with the sharp rise in the ambient temperature after mid-day and the subsequent drop in the ambient temperature after about 2:30 pm. This caused a sharp rise in the panel temperature, especially the uncooled panel, hence the high SD for the uncooled panel. However, the SD in the cooled panel was significantly consistent, this is obviously due to the positive effect of the cooling system on the PV panel. The generally accepted error in temperature measure is up to 8%.

Comparing the results from this study to the reviewed literature as discussed previously shows that, the proposed approach in this study in cooling the PV system is effective and is capable to reduce considerably the temperature of the PV system to enhance its performance.

Around 11:30 am, the temperature of the two panels was assessed using the thermal imager camera, the results for both panels are as indicated in Figure 10. The use of the thermal imager camera is fast and contactless, which enables users to access the temperature of a facility even under operation conditions. It is generally advisable to conduct such an assessment under sunny weather conditions with sun irradiance of at least 600 W/m^2 [10]. The temperature of the panel is visualized to show the distribution of the temperature across the surface of the panel. According to the results from the thermal imager, the temperature distribution does not vary significantly from the results obtained from the thermocouples. The average temperature for the uncooled panel using the thermal imager is 41.28 ◦C compared to the 43.7 ◦C recorded using the thermocouples during the same period. In the case of the cooled panel the average temperature recorded using the thermal imager is 37.8 ◦C compared to 35.72 ◦C recorded using the thermocouples. These differences could be because the thermocouples are closer in terms of contact than the thermal imager and therefore can record more accurately than the thermal imager, also, time differences, i.e., the figures for that of the thermocouples and the thermal imager were not simultaneously recorded. Therefore, time differences could cause the temperature to either increase or decrease slightly based on the ambient temperature at the time. It can be observed from the thermal image for the cooled panel that, the temperature distribution for the panel is relatively uniform obviously due to the coated sheet that was placed on whole panel with uniform temperature distribution. The values on the y-axis in the histogram denote the percentage of temperature distribution on the surface of the panel. This indicate that the temperature of the panel is not equal at every section, certain parts of the module are hotter than others.

4.4. Electrical Efficiency of Panels.

Figure 11 shows the percentage of efficiency gain associated with the temperature change due to passive cooling of the panels by using a low-emissivity coating, which acts as an optical filter that reflects the IR part of the incoming radiation and transmits the visible part

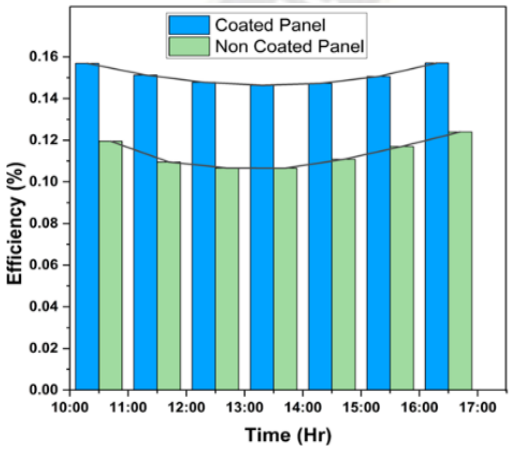

International Journal on Recent and Innovation Trends in Computing and Communication
ISSN: 2321-8169 Volume: 11 Issue: 9
Article Received: *25 July 2023* ***Revised:*** *12 September 2023* ***Accepted:*** *30 September 2023*

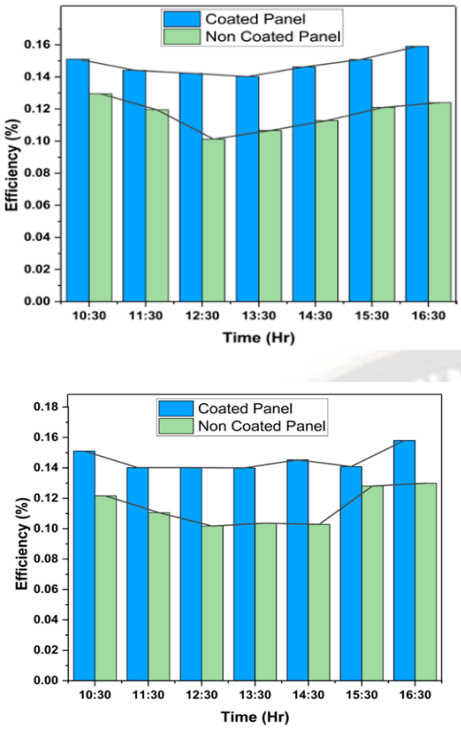

Figure 11. Efficiency comparison for two panels in a month (a) August (b) September (c) October

The percentage of reflection and transmission is not proven here via mathematical modeling, but coating acts as an effective method for passively cooling the panel. The temperature variation is greater in August than in September and October since the temperature variation during August is greater because it is the rainy season and because of the greater duration of cloudy conditions. In the beginning, the efficiency of both panels decreases and reaches its lowest point at noon because the losses are greater due to the increased temperature of the panel. The efficiency started to increase after noon until the readings were recorded. The average efficiency gain for a passively cooled panel for August, September, and October is 3.76 %, 3.13%, and 3.24% compared to the noncooled panel is shown in Figure 11.

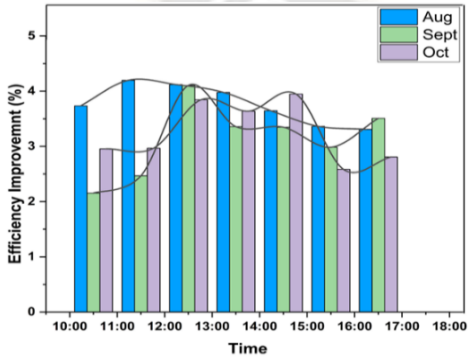

Figure 12. Efficiency improvement in August, September, and October

A comparison of the improvements in efficiency in August, September, and October as shown in Fig.12 revealed that the highest efficiency improvement occurred in August when the value increased by up to 4.19 %. Fluctuations in the curve are observed due to variations in wind speed and seasonal changes occurring in August, September, and October

5. Conclusions

The performance of flexible solar cells decreases significantly as the temperature of the solar cells increases beyond a certain limit.

- The maximum decrease in temperature of the cooled flexible PV panel was decreased by 6-7°C in August compared to the uncooled panel, and an average decrease of 5ºC was observed for this period. The maximum increase in electrical efficiency of the passively cooled PV module was 4.19 % compared to the noncooled panel in August.
- It can be concluded that for every increase of 1 volt in average values of I-V characteristics, there is an associated gain in efficiency of up to 2% for the cooled panel.
- The open-circuit voltage of the cooled panel also increased throughout, thereby increasing the overall power output of the panel. However, the cooled panel showed good stability for I-V characteristics which is a competitive achievement.
- An improvement in efficiency was observed in August, September, and October for the cooled panel over the noncooled panel. The improvement in efficiency reached a maximum value of 4.19 % in August while the average improvement in efficiency was 3.76 % for that month. Similarly, the highest improvement in electrical efficiency for September and October was 4.10 % and 3.94 % respectively. The average improvements in electrical efficiency were observed to be 3.13% for September and 3.24 % for October

The obtained results show that the low-emissivity coating is effective for cooling while being economical at the same time. The manual application of a thin layer coating was seen as efficient. After coating the reduction in transparency was negligible, therefore it can be concluded that the coating enhanced the overall performance of flexible solar cells.

Future studies using different deposition layer techniques and employing multilayer coatings for enhancement of overall performance are required to be analyzed. The resulting material could be integrated with flexible PV panels for actual use during fabrication for passive cooling.

Nomenclature	
FF	Fill factor
I_M	Maximum power output point current (Amp)
I_{SC}	Short-circuit current (Amp)
STC	Standard test condition
V_M	Maximum power output point voltage (V)
V_{OC}	Open-circuit voltage (V)
η	Energy efficiency (%)
η_{ref}	Reference efficiency (%)
T_{ref}	Reference temperature of the PV cells
T_{PV}	Temperature of the PV cells

β_{ref}	Temperature coefficient

Acknowledgements

I acknowledge Defence Laboratory Jodhpur and MBM University Jodhpur who provided me with research facility and kind support throughout my research work. I also Acknowledge my Supervisor Dr. Kamlesh Purohit for his valuable guidance and support for every step of my research.

Conflict of Interest Statement

The Authors declare no conflicts of Interest

References

[1] E. Skoplaki, and J.A. Palyvos, (2009) "On the temperature dependence of photovoltaic module electrical performance: A review of efficiency/power correlations" Solar energy 83(5): 614-624. DOI: https://doi.org/10.1016/j.solener.2008.10.008

[2] G. Notton, C. Cristofari, M. Mattei, and P. Poggi, (2005) "Modelling of a double-glass photovoltaic module using finite differences" Applied Thermal Engineering 25(17-18): 2854-2877. DOI: https://doi.org/10.1016/j.applthermaleng.2005.02.008

[3] F.G. Čabo, and T.G. Marco, (2016) "Photovoltaic panels: A review of the cooling techniques" Transactions of famena 40.

[4] M.W. Edenburn, (1981) "Active and passive cooling for concentrating photovoltaic arrays" 1981 NASA STI/Recon Technical Report, Report No. 82 21745.

[5] K. Araki, H. Uozumi and M. Yamaguchi, (2002) "A simple passive cooling structure and its heat analysis for 500/spl times/ concentrator PV module," Proc. of 2002 Twenty-Ninth IEEE Photovoltaic Specialists Conference, New Orleans, LA, USA, 1568-1571.

[6] J.K. Tonui , and Y. Tripanagnostopoulos, (2007) "Improved PV/T solar collectors with heat extraction by forced or natural air circulation" Renewable energy 32(4): 623-637. DOI: https://doi.org/10.1016/j.renene.2006.03.006

[7] S.A. Kalogirou, (2001) "Use of TRNSYS for modeling and simulation of a hybrid pv–thermal solar system for Cyprus" Renewable energy 23(2): 247-260. DOI: https://doi.org/10.1016/S0960-1481(00)00176-2

[8] Y. Tripanagnostopoulos, T. H. Nousia, M. Souliotis, and P. Yianoulis, (2002) "Hybrid photovoltaic/thermal solar systems" Solar energy 72(3): 217-234. DOI: https://doi.org/10.1016/S0038-092X(01)00096-2

[9] S. Krauter, (2004) "Increased electrical yield via water flow over the front of photovoltaic panels" Solar energy materials and solar cells 82(1-2): 131-137.DOI: https://doi.org/10.1016/j.solmat.2004.01.011

[10] A. Hadipour, M.R. Zargarabadi, and S. Rashidi, (2021) "An efficient pulsed-spray water cooling system for photovoltaic panels: Experimental study and cost analysis" Renewable Energy 164 (2021): 867-875. DOI: https://doi.org/10.1016/j.renene.2020.09.021

[11] A. Kordzadeh, (2010) "The effects of nominal power of array and system head on the operation of photovoltaic water pumping set with array surface covered by a film of water" Renewable energy 35(5): 1098-1102. DOI: https://doi.org/10.1016/j.renene.2009.10.024

[12] E. Cuce, T. Bali, and S. A. Sekucoglu, (2011) "Effects of passive cooling on performance of silicon photovoltaic cells" International Journal of Low-Carbon Technologies 6 (4): 299-308. DOI: https://doi.org/10.1093/ijlct/ctr018

[13] R. Mazón Hernández, J.R. García Cascales, F. Vera-García, A. S. Káiser, and B. Zamora, (2013) "Improving the electrical parameters of a photovoltaic panel by means of an induced or forced air stream" International Journal of Photoenergy 2013: 1-10. DOI: https://doi.org/10.1155/2013/830968

[14] A. Hassan, (2010) "Phase change materials for thermal regulation of building integrated photovoltaics" Ph.D. Dissertation, Technological University, Dublin.

[15] S. Maiti, S. Banerjee, K. Vyas, P. Patel, and P.K. Ghosh, (2011) "Self-regulation of photovoltaic module temperature in V-trough using a metal-wax composite phase change matrix"Solar energy 85(9): 1805-1816. DOI: https://doi.org/10.1016/j.solener.2011.04.021

[16] C.J. Smith, P.M. Forster, and R. Crook, (2014) "Global analysis of photovoltaic energy output enhanced by phase change material cooling" Applied energy 126: 21-28. DOI: https://doi.org/10.1016/j.apenergy.2014.03.083

[17] M. Rosa, P. Rosa, G. M. Tina, and P. F. Scandura, (2010) "Submerged photovoltaic solar panel: SP2 " Renewable Energy 35(8): 1862-1865. DOI: https://doi.org/10.1016/j.renene.2009.10.023

[18] I. Elseesy, T. Khalil, & M.H. Ahmed, (2012) " Experimental investigations and developing of photovoltaic/thermal system" World Applied Sciences Journal 19(9):1342-1347. DOI: https://doi.org/10.5829/idosi.wasj.2012.19.09.2794

[19] M. Chandrasekar, S. Suresh, and T. Senthilkumar, (2013) "Passive cooling of standalone flat PV module with cotton wick structures" Energy Conversion and Management 71(2013): 43-50. DOI: https://doi.org/10.1016/j.enconman.2013.03.012

[20] A.H. Alami, (2014) "Effects of evaporative cooling on the efficiency of photovoltaic modules" Energy Conversion and Management 77 (2014): 668-679. DOI: https://doi.org/10.1016/j.enconman.2013.10.019

[21] X. Han, Y. Wang, and L. Zhu, (2013) "The performance and long-term stability of silicon concentrator solar cells immersed in dielectric liquids" Energy conversion and management 66 (2013): 189-198. DOI: https://doi.org/10.1016/j.enconman.2012.10.009

[22] S.A. Abdulgafar, O. S. Omar and K.M. Yousif, (2014) "Improving the Efficiency of Polycrystalline Solar

Panel Via Water Immersion Method" International Journal of Innovative Research in Science, Engineering and Technology 3 (2014):8127-8132.

[23] Y. Lu, Z. Chen, L. Ai, X. Zhang, J. Zhang, J. Li, W. Wang, R.Tan, N. Dai, and W. Song, (2017) "A universal route to realize radiative cooling and light management in photovoltaic modules" Solar RRL 1(10): p 1700084. DOI: https://doi.org/10.1002/solr.201700084

[24] Z. Zhou, Z. Wang, and P. Bermel, (2019) "Radiative cooling for low-bandgap photovoltaics under concentrated sunlight" Optics Express 27(8): 404-418. DOI: https://doi.org/10.1364/OE.27.00A404

[25] D. Singh, A. K. Singh, S. P. Singh, and S. Poonia, (2020) "Optimization of tilt angles for solar devices to gain maximum solar energy in Indian climate" Proc. of 2020 Advances in Clean Energy Technologies, Springer Singapore, 189-199.

[26] G.J. Jorgensen, S. Brunold, M. Koehl, P. Nostell, H. Oversloot, and A.Roos, (1999) "Durability testing of antireflection coatings for solar applications" Proc. of 1999 Solar Optical Materials XVI, 3789, 66-76.

[27] B.P. Jelle, S. E. Kalnæs, and T. Gao, (2015) "Low-emissivity materials for building applications: A state-of-the-art review and future research perspectives" Energy and Buildings 96 (2015): 329-356. DOI: https://doi.org/10.1016/j.enbuild.2015.03.024

[28] K. Emery, (2007) Standardization News 35(1): 30-33 https://www.researchgate.net/publication/255945173

[29] J.N. Roy, G. R. Gariki, and V. Nagalakhsmi, (2017) "Reference module selection criteria for accurate testing of photovoltaic (PV) panels" Solar Energy 84(1): 32-36. DOI: https://doi.org/10.1016/j.solener.2009.09.007

[30] N.N. Nikitenkov, (2017) Modern technologies for creating the thin-film systems and coatings.1st Ed. IntechOpen, Russia, 2017.

[31] R. Hassan, (2020) "Experimental and numerical study on the effect of water cooling on PV panel conversion efficiency" Proc. of 2020 IOP Conference Series Materials Science and Engineering, Iraq, p. 022094. DOI: 10.1088/1757-899X/928/2/022094

[32] Z.A. Haidar, J.Orfi, and Z. Kaneesamkandi, (2018) "Experimental investigation of evaporative cooling for enhancing photovoltaic panels efficiency" Results in Physics 11 (2018): 690-697. DOI: https://doi.org/10.1016/j.rinp.2018.10.016

[33] V.S. Chandrika, A. Karthick, N.M. Kumar, P.M. Kumar, B. Stalin, M. Ravichandran, Experimental analysis of solar concrete collector for residential buildings, Int. J. Green Energy 18 (2021) 615–623.

[34] D. Pengra, T. Dillman, Notes on data analysis and experimental uncertainty (accessed October 27, 2023), https://courses.washington.edu/phys431/uncertainty_note.pdf.